Parametric analysis of a photonic radiative cooling system

Weimin Wang[1], Nick Fernandez[2] and Srinivas Katipamula[2]

[1] The University of North Carolina at Charlotte, Charlotte (USA)

[2] Pacific Northwest National Laboratory, Richland (USA)

Abstract

Spectrally selective materials show high technical potential for use as radiative cooling heat exchangers for buildings. Recent work by Stanford University has applied a photonic approach to tailor the optical properties of a coating material. In a prototype test, a radiative cooler based on that photonic material has demonstrated the ability to maintain radiator surfaces at below-ambient temperatures in the presence of intense, direct sunlight. This paper presents the simulation and parametric analysis of photonic radiative cooling system that integrates the use of the photonic radiative cooler and radiant floor cooling via the whole energy simulation program EnergyPlus. The simulation was made for a medium office building with three floors and a total floor area of 5,000 m^2. Three key design parameters including the radiator area, the storage tank volume to radiator area ratio, and the water flow rate to radiator area ratio, which are expected to have a large impact on system performance, were investigated in this paper. The results show that the percentage of cooling electricity savings from the photonic radiative cooling system relative to a reference variable-air-volume system has a linear relationship with the radiator area, and a quadratic correlation with the other two variables. The findings from this parametric analysis are valuable to understand how component sizing affects system performance.

Keywords: radiative cooling, parametric analysis, building simulation, nanomaterial

1. Introduction

Space cooling accounts for about 15% of the total primary energy consumed by all commercial buildings in the U.S. (DOE 2011). In the current practice, electricity-driven equipment such as room air conditioners, packaged air conditioners, and chillers are usually the source of mechanical cooling. Although the mechanical cooling equipment can operate reliably to maintain space thermal comfort, they are major energy consumers in buildings. To reduce energy consumption for space cooling, more efforts are needed to utilize passive cooling techniques to replace at least partially the mechanical cooling energy requirement. Possible passive cooling techniques fall into three broad categories (Geetha and Velraj 2012): 1) solar and heat protection techniques to reduce heat gains; 2) heat modulation or amortization techniques to modify heat gains; and 3) heat dissipation techniques to remove heat gains. Radiative cooling belongs to the third category because it uses natural heat sinks (the sky) for heat dissipation.

Radiative cooling refers to the physical process by which a body loses heat to another body of lower temperature via long-wave radiation. In the case of buildings, radiative cooling results from the thermal radiative heat transfer between building surfaces and the colder atmospheric layers in the sky. For a surface with high thermal emittance, the maximum radiative cooling power is about 100 W/m^2 for clear night sky and low ambient relative humidity (Meir et al. 2002). Because of the significant potential of radiative cooling, many studies have been conducted to design suitable materials and systems to make use of radiative exchange with the sky to condition buildings. In general, there are two methods of applying radiative cooling in buildings (Argiriou 2013): passive radiative cooling and active radiative cooling. With passive radiative cooling, the building roof radiates towards the sky and the cooled roof surface temperature then contributes to decreasing the conductive heat gains from the exterior. Representative design strategies of passive radiative cooling include moveable insulation and cool roofs (Al-Obaidi et al. 2014). With active radiative cooling, a heat carrier (air or water) is circulated between the interior spaces and radiative panels on the roof. Example studies on active radiative cooling can be found in (Eicker and

doi:10.18086/swc.2017.17.05 Available at http://proceedings.ises.org

Dalibard 2011, Mihalakakou et al. 1998, Parker 2005). These studies vary with respect to the characteristics of radiative panels, the heat transfer medium used, and the system design.

2. Photonic Radiative cooling

Spectrally selective materials have high technical potential for radiative cooling applications by tailoring the spectral optical properties (e.g., emissivity and reflectivity) of the surface in order to maximize thermal heat losses and minimize absorbed solar radiation. In the context of radiative cooling, heat losses occur in the infrared (IR) wavelength range, for which a 300 K blackbody radiation peaks at approximately 10 microns. The blackbody radiation peak shifts to shorter wavelengths with higher temperatures, but is still in this approximate range for most buildings applications. Spectrally selective materials can potentially offer the capability of daytime radiative cooling, which is highly sought after because of its potential to offset peak cooling loads. However, realizing daytime radiative cooling is severely complicated by both solar irradiance, which peaks at approximately 1,000 W/m^2 between 0.25 and 3 microns (Granqvist 2003), and atmospheric absorption. Without an effective solar irradiation heat shield in place, solar irradiance will easily swamp any radiative cooling effect during most of the day. Atmospheric absorption is problematic in that at many infrared wavelengths, the heat transfer phenomena at a conventional building surface or from radiative panels are closely coupled with the surrounding air (atmosphere is opaque to thermal radiation) and can be further complicated by sky conditions. There is however, a range between 8 to 14 microns where atmospheric absorption is negligible and the buildings thermal radiation can effectively be exchanged with the coldness of outer space. Thus, for optimal cooling, the spectral reflectivity of a building envelope coating would then be (Granqvist 2003):

- $R(\lambda) = 1$ for $0.3\ \mu m < \lambda < 3\ \mu m$ (Daytime radiation shield)
- $R(\lambda) = 0$ for $8\ \mu m < \lambda < 14\ \mu m$ (Thermal emission)

Much of the initial work [e.g., Eriksson and Granqvist 1986, Niklasson and Nilsson 1995) on spectrally selective materials focused on pigments (e.g., ZnS, and ZnO) and sputtered multilayer dielectric films (e.g., MgO, LiF, and oxynitride) on Aluminum backing (infrared reflective). Although such materials are relatively easy to fabricate and deposit, their solar reflectivity is only approximately 80-85%, which means that daytime radiative cooling is not possible, with the exception of early morning or late evening when the solar irradiance is low. Because of the inability of standard materials to meet the strict requirements for daytime radiative cooling, there has been recent research into advanced materials with tailored optical properties to fill the need. These advanced materials are primarily featured of nanomaterials or nanostructured and microstructured thin films (Gentle and Smith 2015, Raman et al. 2014).

The work presented in this paper is based on the nanostructured coatings developed by a research team at Stanford University (Raman et al. 2014). The advanced coatings are made up of seven one-dimensional photonic layers. The incorporation of the micro or nano photonic layers allows the tailoring of the optical properties of the coating in ways not possible with bulk materials. Such a photonic structure has achieved spectrally selective emittance: strongly reflective over visible and near-infrared wavelengths but strongly emissive between 8 and 14 μ (Fig. 1). When exposed to direct sunlight exceeding 850 W/m^2, the photonic radiative cooler maintained its surface temperature 4.9°C below the ambient air.

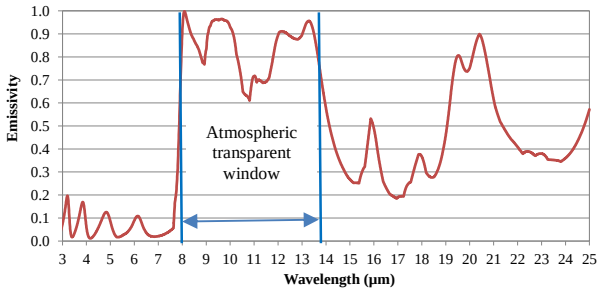

Fig. 1: Photonic material emissivity in the infrared range

3. Photonic radiative cooling System design

It must be noted that the nanostructured coating material studied in this paper is still at the very early research stages. No commercial photonic radiative cooling panels are available, let alone the application of photonic radiative cooling systems in buildings. Many materials presented in the following are more on the conceptual design than the real application design because the focus is to estimate the potential of energy savings from photonic radiative cooling and the associated impact of key design variables.

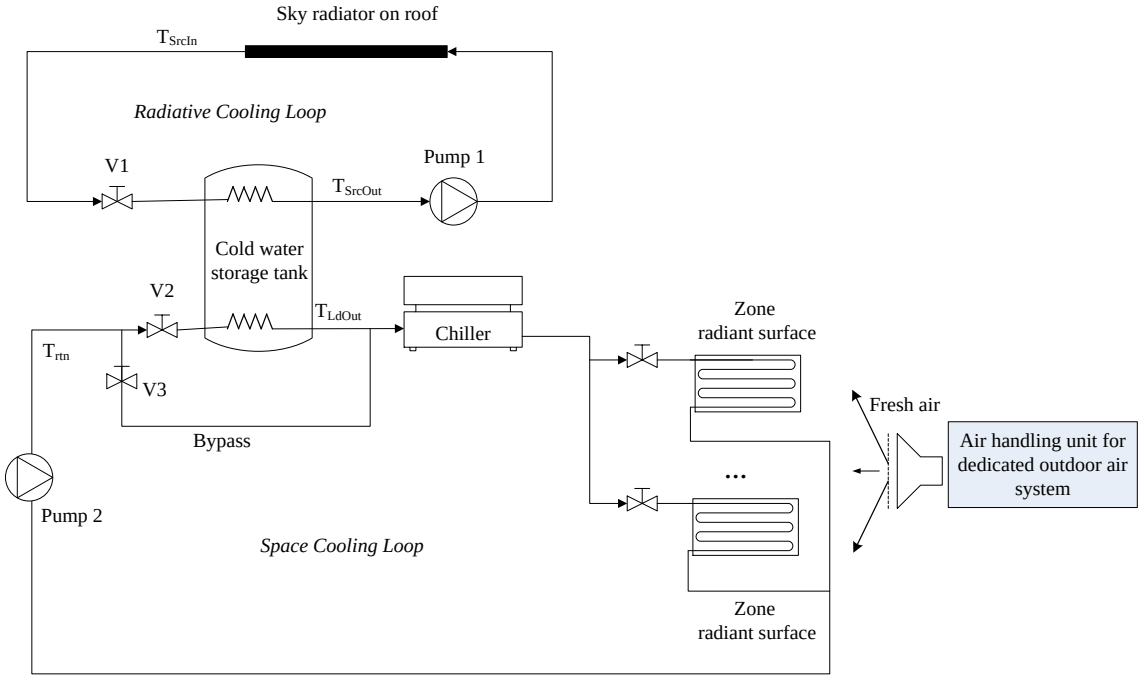

Fig. 2: Schematic diagram of the photonic radiative cooling system

Fig. 2 shows the schematic of the proposed radiative cooling system, which consists of two hydronic loops: a radiative cooling loop and a space-cooling loop. These two loops are coupled via a cold-water storage tank. The radiative cooling loop circulates water through a roof-mounted radiator via a constant-speed pump (Pump 1 in Fig. 2), which draws water from the storage tank and delivers cold water back to the tank. The pump is controlled to run whenever the temperature at the outlet of the radiator (T_{SrcIn}) is lower than the temperature of water at the outlet node of the tank (T_{SrcOut}), subject to the constraint that the loop will not run when the radiator temperature falls below 1°C. The space-cooling loop uses the water storage tank and a supplementary air-cooled chiller to provide cooling. A variable-speed pump (Pump 2 in Fig. 2) serves the space-cooling loop and adjusts the flow as necessary to provide sufficient cooling water to the space. If the outlet tank water temperature for the space cooling loop (T_{LdOut}) is colder than the chilled water temperature set point ($T_{chw,sp}$), i.e., $T_{LdOut} < T_{chw,sp}$, both valves V2 and V3 modulate open, mixing bypassed return water with cold water from the storage tank such that the desired water temperature set point is achieved. Under this scenario, the chiller is not used. If T_{LdOut} is higher than the chilled water return temperature (T_{rtn}), valve V2 closes, the water tank is bypassed, and only the chiller operates to address the cooling load. If $T_{chw,sp} < T_{LdOut} < T_{rtn}$, valve V3 closes and the chiller operates to address the remaining cooling load unmet by the tank.

Because radiative cooling generates cool water at a relatively higher temperature than the chilled water from conventional hydronic systems, it is favorable to employ a zone-level system design that makes use of high-temperature water for cooling. Therefore, as Fig. 2 shows, hydronic radiant floors are used to address the space sensible loads. In the radiant floor design, water tubes spaced at 150 mm are embedded in cement screed for sensible heat exchange with the space. The water tubes are separated from the concrete thermal mass by a 25-mm thick insulation layer (Raman et al. 2014).

To maximize the contribution of radiative cooling, the cold water supplied from the system should be controlled

to run at the highest possible temperature. This minimizes the use of the chiller by bringing the supply-water temperature set point closer to the tank water temperature. To achieve a balance between meeting the space cooling demand and maximizing radiative cooling, the supply-water temperature set point is reset according to the following strategy. If the average temperature for all thermal zones is above the space cooling set point more than 0.27°C, the supply-water temperature set point is decreased at a rate of 2°C per hour. On the other hand, if the average temperature is below the cooling set point more than 0.13°C, the supply-water temperature set point is increased at a rate of 2°C per hour. The supply-water temperature set point is limited to the range between 12.8°C and 18.3°C. Note that the above strategy supply-water temperature reset is based on our engineering experience for this simulation study oriented towards the dry climate in Las Vegas. Refinement and modifications may be needed for real implementations and for different climates.

As mentioned earlier, an air-cooled chiller is used in the photonic radiative cooling system to provide auxiliary cooling whenever the tank water temperature is higher than the supply-water temperature set point. Because of the high supply water temperature, it is desirable to use a low-lift chiller for supplemental cooling, such as that from Katipamula et al. (2010) to achieve superior performance at part load and "low lift" conditions (reduced difference between the entering condenser air temperature and the leaving chilled water temperature). These conditions are representative characteristics of hydronic radiant systems, which use much warmer chilled water temperatures (e.g. ~15°C) than conventional hydronic cooling systems.

A dedicated outdoor air system (DOAS) is used to provide ventilation air to the building in the absence of conventional air-handlers. The DOAS contains a constant volume fan, a hydronic heating coil and a direct-expansion cooling coil for air conditioning. The supply-air temperature set point of the DOAS is set at 12.8°C when the outdoor-air temperature is higher than 16°C, 18°C when the outdoor-air temperature is lower than 10°C, and linearly between the above boundary set points when the outdoor-air temperature lies in the range between 10°C and 16°C.

Regarding the sky radiator on roof (Fig. 3), it is conceptualized as a flat, metallic plate with its surface covered with the nanostructured, spectrally selective coating material as described in the previous section. Underlying the surface layer is an array of metallic piping, welded to the underside of the top plate. Each pipe runs parallel from an inlet manifold on one side of the radiator and returns to an outlet manifold on the other side of the radiator. The spacing between pipes is 150 mm (6 in.) and the pipe diameter is 19 mm (0.75 in.). Water pipes are located in-between the radiative cooler and a thin thermal conductive layer (e.g., aluminum plate). The sky radiator is integrated with the roof construction. To mitigate the convective heat gains from the surrounding, the photonic radiative cooler (Fig. 3) is covered with a 25-μm low-density polyethylene film and there is a 25 mm air space in between them. The use of polyethylene film follows the prototype design by the photonic radiative cooling material developer (Raman et al. 2014).

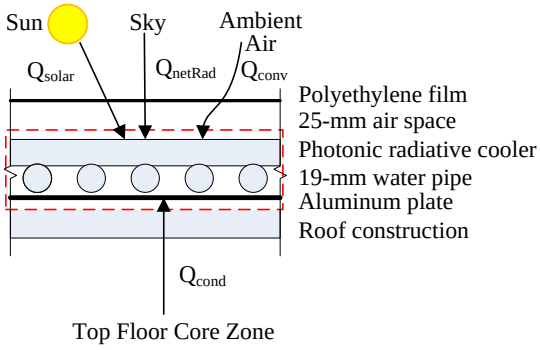

Fig. 3: Roof-integrated photonic radiator design

4. Building Model and Reference System

The building model originated from the Building Energy Codes Program (DOE 2015), which maintains a series of EnergyPlus models in compliance with different versions of commercial codes. A prototype medium-sized office building was used for the parametric analysis. The building (Fig. 4) has three floors and a total floor area of about 5000 m^2. The building has a rectangular shape with an aspect ratio of 1.5. Windows are distributed evenly

in continuous ribbons around the perimeter of the building. The window fraction of the overall façade area is 33%. The building construction includes steel-framed walls, a flat roof with insulation above the deck, and a slab-on-grade concrete floor. The performance values of the exterior envelope meet the minimum requirement of ASHRAE Standard 90.1-2013 (ASHRAE 2013). More detailed description about the building model including thermal zoning and internal loads can be referred to Thornton et al. (2011).

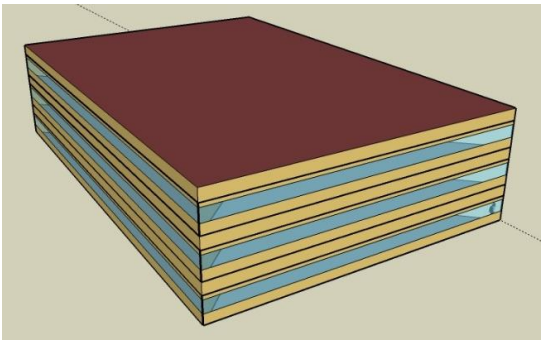

Fig. 4: Axonometric view of the medium office building

To investigate the impact of different design parameters of the photonic radiative cooling system on building energy consumption, we defined a reference system to represent the prevailing technology used to condition medium-sized office buildings. With a reference system, the potential of energy savings from different design scenarios of the photonic radiative cooling system can be conveniently derived and compared in a straightforward manner. The reference has an individual variable-air-volume (VAV) system for each floor (Fig. 5). All equipment types, efficiency, and system design features followed Standard ASHRAE 90.1-2013. The building model is essentially the same as the original source (DOE 2015) except for one change. The original source used the mean air temperature to define the heating and cooling set points at 21°C and 24°C, respectively. They were changed to use operative temperature for thermal comfort, with heating set point at 21.6°C and cooling set point at 25.7°C. Such a change is necessary to make a fair comparison between the VAV system and the photonic radiative cooling system. The use of hydronic radiant floors is favorable for occupant thermal comfort because of its higher floor temperature for heating and lower floor temperature for cooling relative to the VAV system.

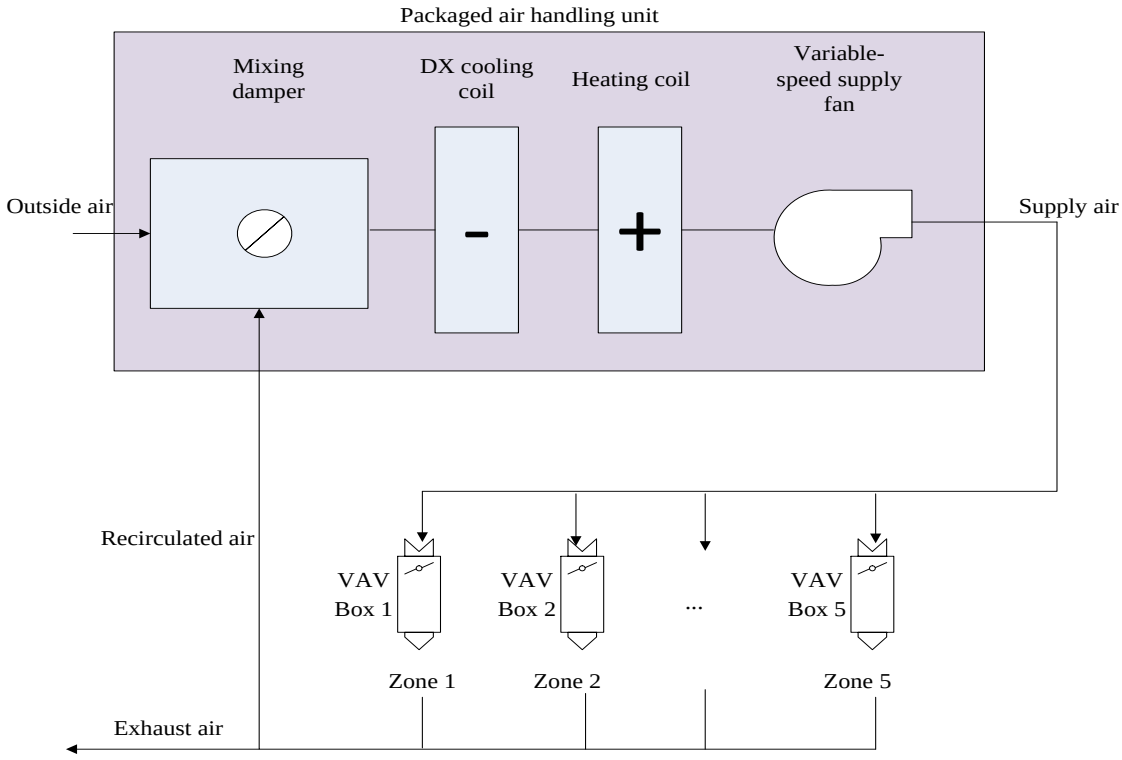

Fig. 5: Schematic diagram of the reference VAV system for each floor

5. System Modeling and Simulation Matrix

The photonic radiative cooling system, the reference VAV system, and the building were all simulated with EnergyPlus, a dynamic, whole building simulation program that supports a large variety of mechanical systems and components. Because there is no existing object in EnergyPlus for the novel photonic radiator, the energy management system (EMS) module in EnergyPlus was used to create a user-defined model of the radiator that is directly interfaced with the rest of the hydronic system specified in EnergyPlus. The EMS supports a simple programming language through which the user can construct new models and customize control sequences. To calculate the expected outlet temperature from the rooftop radiator and the average temperature of the radiator, the rooftop radiator was modeled in the EMS as a discretized heat exchanger by dividing the radiator into a discrete number of segments (Fig. 3 shows on segment as enclosed in the dashed lines). Heat transfer processes involved in the modeling of the photonic radiator includes the following:

- Absorbed solar radiation (Q_{solar}, W/m^2);
- Conduction (Q_{cond}, W/m^2) heat transfer between the underside of the radiator and the underlying building roof;
- Convection (Q_{conv}, W/m^2) heat transfer between the upper radiator surface and the ambient air; and
- Net longwave radiation (Q_{rad}, W/m^2) heat transfer between the upper radiator surface and the sky, which combines the outgoing longwave radiation emitted from the radiator minus the downward radiation from the sky absorbed by the radiator.

Detailed modeling of the photonic radiative cooler and the strategies used for the system simulation were reported in a previous paper (Wang et al. 2016) and are no longer repeated here.

Many design variables potentially affect the performance of the photonic radiative cooling system. Examples of those design variables include the sky radiator area, the tank size, the water flow rate in the radiative cooling loop, the system control variables (e.g., the supply water temperature), and building design variables (e.g., building location, area, and envelope thermal resistance). Recognizing that performing an exhaustive parametric analysis is resource-prohibitive, we decided to select the following three variables for further parametric analysis: the sky radiator area, the cold-water storage tank size, and the cold-water flow rate in the radiative cooling loop. These

three variables were thus selected because they are usually regarded as the key variables to be considered for a radiative cooling system design. Both the baseline values and the perturbed values of these three variables are discussed below.

The sky radiator area directly affects the amount of free cooling that the system can provide. A larger radiator area can generate more cooling but also implies a higher initial cost. In addition, practical constraints may apply for the area of roof-integrated radiators because the existence of mechanical equipment, ventilation and roof access infrastructure makes it unrealistic to cover the entire roof with the radiative panels. In the baseline mode, the sky radiator is assumed to occupy 50% (i.e., 830 m^2) of the roof area. Additional values studied for the parametric analysis include 30% (498 m^2), 40% (664 m^2), 60% (996 m^2), and 70% (1163 m^2) of the roof area.

The cold-water storage tank plays an important role in the system as the mismatch (temporal or magnitude) between radiative cooling capacity and space cooling load is common throughout the whole year. However, no practical design guide was found to determine the optimal size of tank storage. Eicker and Dalibard (2011) used a 1.2 m^3 storage tank for a net-zero home with a radiator area of 38 m^2. We simply scaled up the tank size following the same storage tank volume to radiator area ratio (i.e., 1200 L/38 m^2 = 31.6 L/m^2), which ends up with a tank volume of 26.2 m^3 in the baseline model. In the parametric analysis, the tank size was perturbed to take 50%, 75%, 125%, and 150% of the baseline value, which has the storage tank volume to radiator area ratio of 15.8 L/m^2, 23.7 L/m^2, 39.4 L/m^2, and 47.3 L/m^2, respectively.

The cold-water flow rate was also explored in the parametric analysis to investigate its impact on system performance. The baseline model had a cold-water flow rate at 26 kg/h per m^2 of radiator area. In the parametric analysis, the cold-water flow rate was perturbed to take 50%, 75%, 125%, and 150% of the baseline value, which respectively corresponds to 13.0 kg/h, 19.5 kg/h, 32.5 kg/h, and 39.0 kg/h per m^2 of the radiator area.

Tab. 1 summarizes the parameter values used in the baseline design as well as 12 other parametric models. It needs to be noted that in each run, a single variable was perturbed in the parametric analysis, relative to the baseline. Multi-variable parametric analysis is left for future work.

Tab. 1: Simulation runs for parametric analysis

Run	% of roof area used for radiator	Storage tank volume to radiator area ratio (L/m^2)	Water flow rate to radiator area ratio ($kg/h/m^2$)
1 (baseline)	50%	31.6	26.0
2	60%	31.6	26.0
3	70%	31.6	26.0
4	40%	31.6	26.0
5	30%	31.6	26.0
6	50%	15.8	26.0
7	50%	23.7	26.0
8	50%	39.4	26.0
9	50%	47.3	26.0
10	50%	31.6	13.0
11	50%	31.6	19.5
12	50%	31.6	32.5
13	50%	31.6	39.0

6. Simulation Results and discussion

All simulation runs shown in Table 1 were made for the location of Las Vegas, NV. Simulation results are discussed below.

As Fig. 2 shows, the sky radiator provides cooling and thereby reduces the time needed to run the electric chiller. Therefore, in comparison with the reference VAV system, the photonic radiative cooling system saves the

electricity for cooling, saves the fan energy, but also introduces additional pump energy as needed by the hydronic system. We will focus on the cooling electricity savings only because 1) fan energy savings is mainly due to the use of DOAS, which is not exclusive to photonic radiative cooling; and 2) the pump energy is negligible in comparison with cooling energy.

Fig. 6 shows the impact of sky radiator area on cooling electricity savings. The following can be seen from this figure:

- Relative to the reference VAV system, the photonic radiative cooling system saved 42% cooling electricity for the case of sky radiator occupying 50% of the roof area. The percentage of savings increased by 2% as the roof area used for the sky radiator increased by every 10%.
- There is a linear relationship between the percentage of cooling electricity savings and the percentage of roof area for radiative panels. Eq. 1 is the linear regression derived from the five sets of data with different radiator areas.

$$PerClgElec=0.204*PerRA+0.317 \quad \text{(eq. 1)}$$

where, $PerClgElec$ is the percentage of cooling electricity savings of the photonic radiative cooling system, and $PerRA$ is the percentage of roof area used for radiative panels.

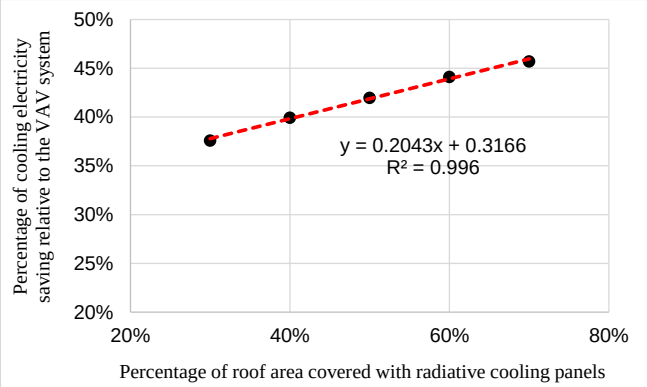

Fig. 6: Impact of radiator area on cooling electricity savings

Fig. 7 shows the impact of tank size on cooling electricity savings. This figure indicates that:

- Relative to the reference VAV system, the photonic radiative cooling system saved 42% cooling electricity for the case of baseline design of the cold-water storage tank size. The percentage of savings increased to 42.7% and 43.3% if the tank volume to radiator area ratio (VAR, L/m^2) was increased to 39.4 L/m^2 and 47.3 L/m^2. The percentage of savings decreased to 38.8% and 40.7% if the VAR was decreased to 15.8 L/m^2 and 23.7 L/m^2.
- The marginal benefit decreases with the increase of tank size. It is reasonable to expect that the cooling electricity savings will reach to a peak at certain value of VAR, beyond which no marginal benefit can be achieved.
- A quadratic correlation exists between the percentage of cooling electricity savings and the tank volume to radiator area ratio. Eq. 2 is the regression derived from the five sets of data with different values of VAR.

$$PerClgElec=-0.00004*VAR^2+0.0037*VAR+0.3394 \quad \textit{(eq. 2)}$$

Fig. 8 shows the impact of the water flow rate to radiator area ratio on cooling electricity savings. This figure shows that:

- The percentage of cooling electricity savings increased from 42% to 44% if the water flow rate to radiator area (FAR, kg/h/m^2) was decreased from 26 kg/h/m^2 for the baseline by half to 13 kg/h/m^2. No evident change of cooling electricity savings was observed if the FAR was increased from the baseline.

- A quadratic correlation also exists between the percentage of cooling electricity savings and the water flow rate to radiator area ratio. Eq. 3 is the regression derived from the five sets of data with different values of FAR.

$$PerClgElec=0.000005*FAR^2 - 0.0036*FAR+0.4753 \quad \text{(eq. 3)}$$

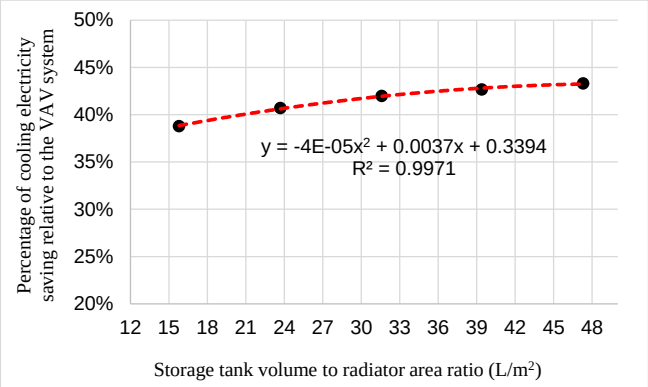

Fig. 7: Impact of storage tank volume to radiator area ratio on cooling electricity savings

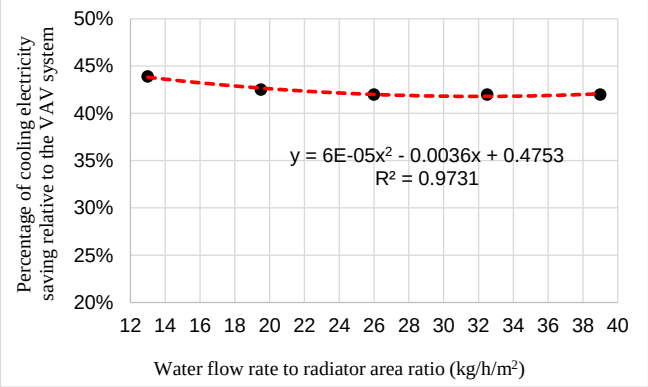

Fig. 8: Impact of water flow rate to radiator area ratio on cooling electricity savings

The difference of cooling electricity savings is attributable to the capacity of radiative cooling relative to the system cooling demand. As Fig. 2 shows, the water returned from radiant floors is cooled by the storage tank or the air-cooled chiller. The tank cooling energy is from the radiative cooler, so it can be regarded as "free" energy. For the photonic radiative cooling system, the percentage of free energy used to address the cooling load for each month is illustrated in Fig. 9 and Fig. 10, respectively illustrating the impact of radiator area and storage tank volume to radiator area ratio. The results for flow rate to radiator area ratio is not shown because of its minor impact on cooling electricity.

Fig. 9 and Fig. 10 show the following:

- For both cases, the percentage of "free" cooling from the sky radiator was the lowest in the summer months when there was a higher cooling load and a lower radiative cooling potential.
- As expected, the percentage of free radiative cooling increased with the sky radiator area (Fig. 9) and the tank size (Fig. 10).
- The percentage of free radiative cooling is less sensitive to the tank size than to the radiator area. Over all 12 months, the average difference of cooling electricity savings is 14% by changing the sky radiator area from 30% to 70% of roof area, while it is about 9% by changing the storage tank volume from 50% to 150% of its baseline design.

- For the baseline model, the free cooling from the sky radiator is can satisfy more than 90% of the entire building cooling load in January, February, March, November, and December. Such observation still holds true when the sky radiator area is reduced down to 30% of the roof area.

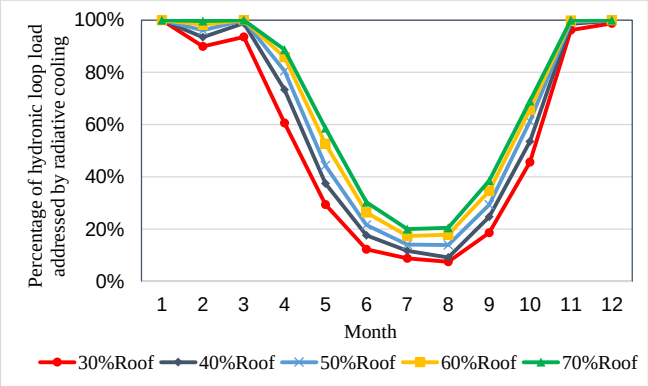

Fig. 9: Percentage of free cooling relative to radiator area

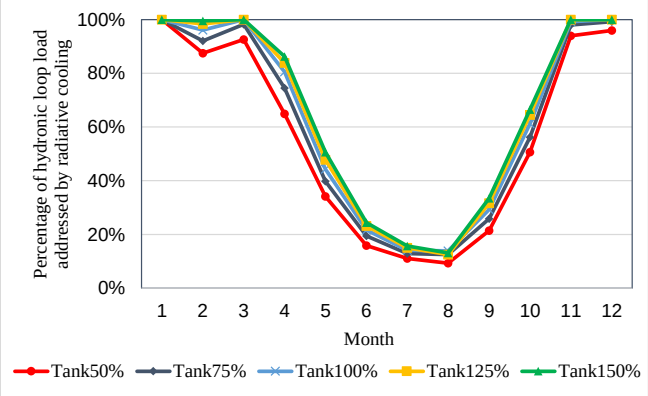

Fig. 10: Percentage of free cooling relative to tank volume to radiator area ratio

It needs to be noted that the electricity savings presented in this section should be interpreted as the outcome of system change, instead of the photonic radiative cooler only. The technical report (Fernandez et al. 2015) can be referred to for the benefits of the photonic radiative cooling system in comparison with other alternative systems (e.g., hydronic radiant systems and nighttime radiative cooling systems). In addition, using the regression equations to extrapolate results beyond the ranges investigated in this work may be questionable.

7. Conclusions

The photonic radiative cooling system has a great potential in building applications to save cooling electricity, compared to typical VAV systems for office buildings. The detailed energy simulation showed that for a three-floor medium office building located in Las Vegas, a baseline design of the photonic radiative cooling system with 50% of the roof area used for radiator and cold water storage tank sized at 31.6 L per m^2 of radiator area saved 42% cooling electricity relative to the reference VAV system. Based on a parametric analysis for three key design parameters, namely the radiator area, the storage tank volume to radiator area ratio (VAR), and the water flow rate to radiator area ratio (FAR), the simulation results revealed that the percentage of cooling electricity savings had a linear relationship with the radiator area, and a quadratic relationship with both VAR and FAR. The percentage of savings increased by 2% as the roof area used for the sky radiator increased every 10%. The marginal benefit decreased with the increase of storage tank volume to radiator area ratio. The cooling electricity savings decreased by if the flow rate to radiator area ratio was increased from 13 kg/h/m^2 to 26 kg/h/m^2, beyond which there is no change of electricity savings. The percentage of free radiative cooling increased with the sky radiator area and the tank size. The percentage of free radiative cooling is more sensitive to the radiator area than to the

storage tank volume to radiator area.

Further investigation can be made for other variables such as the radiator orientation if standalone sky radiator is used. Design optimization of multiple variables is also worth considering in future work.

ACKNOWLEDGMENTS
The work was funded by the Building Technologies Office of the U.S. Department of Energy.

REFERENCES

Al-Obaidi K.M., Ismail, M., Rahman, A.M.A., 2014. Passive cooling techniques through reflective and radiative roofs in tropical houses in Southeast Asia: A literature review. Frontiers of Architectural Research, 3(3), pp. 283-297

Argiriou A., 2013. Radiative cooling, in: Santamouris, M. and Asimakopoulos, D. (Eds.), Passive Cooling of Buildings, Earthscan New York, pp. 424-454.

ASHRAE, 2013, ANSI/ASHRAE Standard 90.1-2013: Energy Standard for Buildings Except Low-Rise Residential Buildings, American Society of Heating, Refrigerating and Air Conditioning Engineers, Inc., Atlanta, GA.

DOE, Department of Energy, U.S., 2011. Building Energy Data Book, http://buildingsdatabook.eren.doe.gov/, Accessed in June 2017

DOE, 2015. Commercial Prototype Building Models. Building Energy Codes Program, Department of Energy, https://www.energycodes.gov/commercial-prototype-building-models, Accessed in June 2017

Eicker U., and Dalibard, A., 2011. Photovoltaic-thermal collectors for night radiative cooling of buildings. Solar Energy, 85(7), pp.1322-1335.

Eriksson T.S., Granqvist, C.G., 1986. Infrared properties of Silicaon Oxynitride Filens: experimental data and theoretical interpretation. Journal of Applied Physics (60):2081.

Fernandez N., Wang, W., Alvine K.J., Katipamula, S. 2015. Energy Savings Potential of Radiative Cooling Technologies. PNNL-24904, Pacific Northwest National Laboratory, Richland, WA.

Geetha N.B., Velraj, R., 2012. Passive cooling methods for energy efficient buildings with and without thermal energy storage – A review. Energy Education Science and Technology Part A: Energy Science and Research, 29(2), pp. 913-946.

Gentle A.R., Smith, G.B., 2015. A subambient open roof surface under the mid-Summer sun. Advanced Science, 2(9):1500119. DOI: 10.1002/advs.201500119

Granqvist C.G., 2003. Solar energy materials. Advanced Materials 15(21):1789-1803.

Katipamula S., Armstrong, P., Wang, W., Fernandez, N., Cho, H., Goetzler, W., Burgos, J., Radhakrishnan, R., and Ahlfeldt, C., 2010. Development of High-Efficiency Low-Lift Vapor Compression System - Final Report. Technical Report PNNL-19227, Pacific Northwest National Laboratory, Richland, WA.

Meir M.G., Rekstad, J.B., Lovvik, M., 2002. A study of a polymer-based radiative cooling system. Solar Energy, 73(6), pp. 403-417.

Mihalakakou G., Ferrante, A., Lewis, J.O., 1998. The cooling potential of a metallic nocturnal radiator. Energy and Buildings, 28(3), pp. 251-256.

Niklasson G.A., Nilsson T.M.J., 1995. Radiative cooling during the day: simulations and experiments on pigmented polyethylene cover foils. Solar Energy Materials and Solar Cells 37(1): 93-118.

Parker D., 2005. Theoretical Evaluation of the NightCool Nocturnal Radiation Cooling Concept. Technical Report No. FSEC-CR-1502-05, Florida Solar Energy Center, Cocoa, FL.

Raman A.P., Anoma, M.A., Zhu L., Raphaeli E., Fan, S. 2014. Passive radiative cooling below ambient air temperature under direct sunlight. Nature (515):540-544.

Thornton B.A., Rosenberg, M.I., Richman, E.E., Wang, W., Xie, Y., Zhang, J, Cho, H., Mendon, V.V., Athalye, R.A., Liu, B., 2011. Achieving the 30% Goal: Energy and Cost Savings Analysis of ASHRAE Standard 90.1-2010. Technical Report PNNL-20405, Pacific Northwest National Laboratory, Richland, WA.

Wang W., Fernandez, N., Katipamula, K., 2016. Modeling and simulation of a photonic radiative cooling system. Proceedings of the ASHRAE and IBPSA-USA SimBuild Conference, Salt Lake City, UT.